Master's Thesis of Kyeong Pyo Lee

Gyro-kinetic study of residual zonal flow for slowing down distribution function

속도감소 분포함수를 사용한 residual zonal flow의 자이로-운동학적인 연구

August 2017

Graduate School of Engineering Department
Seoul National University
Nuclear Engineering Major

Full Name of you

Gyro-kinetic study of residual zonal flow for slowing down distribution function

Taik Soo Hahm

Submitting a master's thesis of Public Administration

August 2017

Graduate School of Engineering Department
Seoul National University
Nuclear Engineering Major

Kyeong Pyo Lee

Confirming the master's thesis written by
Kyeong Pyo Lee

Month Year

Chair _____(Seal)
Vice Chair _____(Seal)
Examiner _____(Seal)

Abstract

In the burning plasma, fusion reaction produces fast alpha particles for which the production energy is about 3.5 MeV. They saturate to equilibrium by slowing down collisional process, and the equivalent temperature of alpha particle is much greater than that of ion. It suggests that the alpha particle gyro-radius is large compared to ions, and its contribution to zonal flow gets larger in the long wavelength regime. In the previous research, residual zonal flow level (and also zonal flow itself) is calculated in the Maxwellian equilibrium. However, for alpha particle, the equilibrium distribution function is different from the Maxwellian distribution. Hence, the research of residual zonal flow level for slowing down distribution is needed.

In this study, we calculated the residual zonal flow level of alpha particle using slowing down distribution function. In this procedure, we use modern gyro-kinetic pull-back transformation method for residual zonal flow calculation. The results are compared with those obtained in the equivalent Maxwellian distribution function and those of plasma ion. Finally, the combined version of residual zonal flow level is introduced and be compared with the different initial particle energy

Keyword : residual zonal flow, slowing down distribution, alpha particle
Student Number : 2015-21326

Contents

1 Introduction

Turbulent transport in tokamak plasma is a key issue in the magnetic confinement fusion research, since it is considered as a main cause of the anomalous transport which reduces the confinement efficiency of fusion devices. Many studies therefore were performed to understand the plasma turbulence and transport driven by it. Especially theoretical and simulation studies on drift wave turbulence such as ion temperature gradient (ITG) mode have revealed some important aspect of nonlinear dynamics of turbulent transport.

Zonal flow, an axisymmetric low frequency potential fluctuation, is now well known to play a key role of turbulence regulation in the tokamak plasma. It is driven by turbulent Reynolds stress[3]. ExB flow can decorrelate the radial length of turbulent eddies by its radial ExB shear and therefore reduce the plasma turbulence. Extensive simulation studies on drift wave turbulence have shown that turbulence gets saturated nonlinearly due to the zonal flow. Thus, understanding the behavior of zonal flow in the fusion plasma is important.

Residual zonal flow is one of the most interesting characteristics of zonal flow. It is a long time asymptotic response of initially excited fluctuation. When the zonal flow is initially excited, it gets damped by collisionless transit magnetic pumping[18]. However Rosenbluth and Hinton[17] have shown that it does not fully decay but asymptotes to some finite residual level due to the polarization shielding. They calculated this level in the long wavelength limit, and the result is now called "Rosenbluth Hinton residual zonal flow (RH flow)". Further theoretical progress has been made on this issue. Jenko et.al[15] reported their gyro-kinetic simulation results that the residual zonal flow is enhanced in the short wavelength regime. Xiao and Catto[22] confirmed this result from their theoretical study. Wang and Hahm[20] have derived an analytic formula of the residual zonal flow level which is valid in the arbitrary wavelength regime

using modern gyrokinetic approach[6],[10]. However, all aforementioned previous studies were performed assuming the Maxwellian equilibrium distribution. Considering a burning plasma such as ITER and beyond, alpha particles will be produced due to fusion reaction and one should consider the slowing down distribution as an equilibrium distribution. Therefore, zonal flow study for slowing down distribution is needed.

In the present paper, we investigate the residual zonal flow for slowing down distribution using modern gyro-kinetic approach. We start from the expression of the classical and neoclassical polarization density which result from the pullback transformation from gyro-center coordinate to particle coordinate and from bounce gyro-center coordinate to gyrocenter coordinate, respectively. The classical polarization is calculated via a semi-analytic approach in two limiting cases of the zonal flow radial scales. For the neoclassical polarization part, both trapped and passing particle contributions are considered in three limiting cases. Then we calculate the residual zonal flow for the slowing down distribution function and compare the result with the equivalent Maxwellian case. We find that residual zonal flow for slowing down case is higher than that for equivalent Maxwellian distribution in the intermediate radial wavelength range on the order of ion poloidal gyroradius, $k_r \cdot \rho_{\theta i} \sim 1$.

The remainder of this paper is organized as follows. In Section 2, we introduce the theoretical background of our research including the introduction of zonal flow, modern gyro-kinetic formalism, and slowing down distribution. It includes the details of Lie perturbation transformation, polarization density, and slowing down process due to the beam-electron collisions. In section 3, precedent studies of residual zonal flow are shown and demonstrated. Then, detailed calculation of classical and neoclassical polarization density is presented in Section 4. Section 5 illustrates the result of residual zonal flow level for the slowing down

distribution. It is compared with the equivalent Maxwellian case. In addition, initial particle energy dependency of residual zonal flow is demonstrated on this section. Finally, we summarize our work and discuss its possible application in Section 6.

2 Theoretical Background

In this section, we introduce the theoretical background of this residual zonal flow study. The concept of zonal flow and residual zonal flow is briefly demonstrated in section 2.1 and 2.2. Then the gyro-kinetic formalism is introduced in section 2.3, including the concept of conventional gyro-kinetic formalism and modern gyro-kinetic formalism. Finally the slowing down distribution is demonstrated in Section 2.4.

2.1 Zonal flow

The fundamental reason of the residual zonal flow study is that zonal flow is a key element of plasma turbulence dynamics. As mentioned above, zonal flow not only regulates the turbulent transport by its flow shear but also plays an important role of H-mode tokamak operation. In this section, we demonstrate the basic concepts of zonal flow focused on the theoretical description.

2.1.1 basic concept

Zonal flow is, in general, azimuthally symmetric flow structure. The zonal flow appears in various forms in nature and laboratory, and can be observed in the earth's jet stream or the solar dynamo system. In plasma physics, it refers to an low frequency axisymmetric fluctuating field structure which is constant along a magnetic surface. The associated ExB flow is in the poloidal direction, and its direction depends on the sign of potential. The important thing is,

zonal flow regulates turbulence by its flow shear, despite its being built from turbulence, which makes zonal flow the current greatest concern.

2.1.2 formation of zonal flow

The zonal flow basically has a constant electrical potential with respect to the magnetic surface, so that m, n, and $k_{\|}$ are both zero. Because $k_{\|}$ is zero, it no longer follows the Boltzmann response, and the density perturbation is balanced with the linear polarization drift. The zonal flow is a flow structure with a linear dispersion relation of w = 0. The ExB flow created by combining with the B field in Tokamak has a binormal direction by default. Among them, the toroidal component compresses the plasma, and the plasma sends a return flow toward the field line to maintain the incompressibility and eventually forms the poloidal ExB flow. Fig. 1 [2] shows the poloidal direction and toroidal direction components of ExB flow induced by zonal flow, respectively. This flow pattern produces a radial shear of poloidal flow according to the radial variation of the fluctuating field. Fig. 2 [2] shows that the vortex decorrelates with the effect of shearing. In this way, the flow shear tears the turbulent eddy in the radial direction to inhibit turbulent transport.

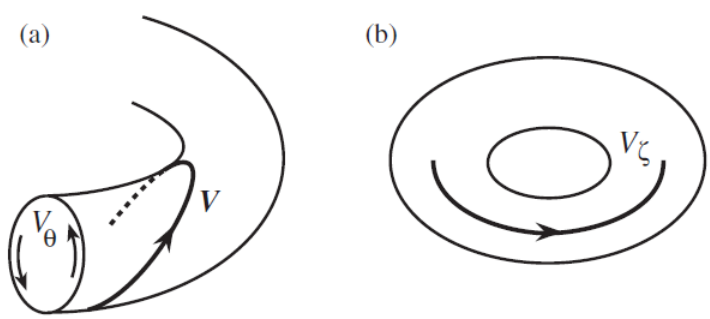

Figure 1: Poloidal(a) and toroidal(b) component of zonal flow.

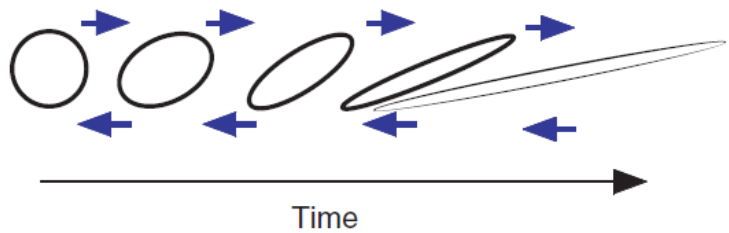

Figure 2: Poloidal(a) and toroidal(b) component of zonal flow.

The zonal flow is basically a linearly stable plasma eigenmode for low frequency electric field perturbation. For Tokamak plasma, there are two relevant solutions as possible modes. One is a slow varying response which satisfies $|\partial/\partial t| \ll \omega_t \, (= v_{Ti}/qR)$. In this case, plasma is incompressible and the ExB flow is associated with a toroidal return flow. The other shows a time transit of (expression) with fast varying response. In this case, plasma compression occurs due to the poloidal asymmetry of the tokamak plasma. Also, the mode is generated from the linear coupling of sideband perturbation which is m = 1, n = 0 resulting from the toroidicity of the field potential of m = n = 0. This is called "Geodesic Acoustic mode (GAM)". In other words, the whole zonal flow consists of slow varying component and GAM.

2.1.3 suppression of turbulence

The most significant characteristic of zonal flow is that zonal flow regulates the turbulence by its flow shear. In magnetized plasmas, if there is flow shear together with the gradient source of turbulence such as pressure gradient the flow shear can suppress the turbulence by gradient relaxation. As zonal flow itself is generated from the turbulence, its regulation of turbulence is balanced with the linear instability. As a result, it constructs the feed-back loop between turbulence and zonal flow and the system is saturated to a certain turbulent

state and transport. The details of the mechanism is described in many fabulous studies[2],[1],[11],refLH1998. Here, we introduce a brief explanation of some key processes during this nonlinear saturation.

The first part we account on is the effect of sheared flow on linear stability, referred in [2]. The linear stability driven by gradient source grows the seed perturbation. If there exists a sheared flow in the turbulent system, the eigenmodes are deformed and distorted from its original direction of the gradient. Thus, the most unstable mode gets stabilized and the linear growth rate decreases. It is very close to the Richardson problem which shows the balance of buoyancy and shearing. As Richardson number is a criterion of dynamics stability of turbulent system, ExB shearing rate of zonal flow determines the stability of linear mode.

Another stabilizing effect is related to the decorrelation of turbulent eddy. Turbulent state of plasma with characteristic Following the Hahm and Burrells equation[11], the fluctuating field $\delta\xi$ is convected by the equilibrium flow $V_0 = V_E + V_{\|}\hat{b}$ and the fluctuating ExB flow $\delta V_E = B \times \nabla\delta\phi/B^2$,

$$\left(\partial/\partial t + V_0 \cdot \nabla + \delta V_E \cdot \nabla\right) \delta\xi\left(\psi, \theta, \chi\right) = S \tag{1}$$

where V_E is the mean ExB flow and $V_E = E_r^{(0)} \times B/B^2$, S is the driving source of the turbulence. To identify the evolution of turbulent structure, two-point correlation equation is derived in the relative coordinates (x_-, v_-),

$$\left(\frac{\partial}{\partial t} + v_- \frac{\partial}{\partial x_-} - \frac{\partial}{\partial v_-} D_- \frac{\partial}{\partial v_-}\right) \langle \delta\xi(1)\delta\xi(2)\rangle = S_2, \tag{2}$$

where S_2 is two-point source term. Here, two point correlation function $\langle\delta\xi\delta\xi\rangle$ is propagating with the relative diffusion coefficient D_-. In the tokamak bal-

looning geometry (ψ, η, χ), the relative diffusion is described as,

$$D_{-}^{eff} = 2D^{eff}\{\left(\frac{\psi_{-}}{\Delta\psi_0}\right)^2 + \left(\frac{\eta_{-}}{\Delta\eta_0}\right)^2 + \left(\frac{\chi_{-}}{\Delta\chi_0}\right)^2\}. \tag{3}$$

By taking various moments, one can find the coupling of flow shear and turbulent diffusion in the decorrelation dynamics. After some calculation[11], the radial correlation length is determined by the decorrelation rate of ambient turbulence $\Delta\omega_T$ with the reduced level,

$$\left(\frac{\Delta\psi_0}{\Delta\psi}\right)^2 = 1 + \frac{\omega_s^2}{\Delta\omega_T^2} \tag{4}$$

where the shearing ω_s is

$$\omega_s^2 \sim \left(\frac{\Delta\psi_0}{\Delta\chi}\right)^2 |\frac{\partial^2}{\partial\psi^2}\phi(\psi)|^2 \tag{5}$$

Therefore, one can say that the radial wavlength of fluctuation is suppressed when the shearing rate exceeds the turbulent decorrelation rate.

2.2 Residual zonal flow

As mentioned above, a deeper understanding of zonal flow is required for tokamak operation, and various studies on the characteristics of zonal flow have been performed. In particular, the damping of the zonal flow has been studied extensively on the temporal behavior of the zonal flow. Many studies have been performed for linear damping of zonal flow on both collisional[14],[8] and collisionless cases[19],[22],[8]. In particular, Rosenbluth and Hinton[17] showed that the zonal flow formed in the Ion Temperature Gradient (ITG) turbulence was not completely attenuated but partially survived by linear collisionless damping based on the gyro-kinetic theory. It has been shown analytically that the

saturated zonal flow level is associated with neoclassical polarization shielding caused by bounce orbit motion due to magnetic geometry in the tokamak. Especially, the result has an approximation,

$$\frac{\phi_k\left(t=\infty\right)}{\phi_k\left(t=0\right)}=\frac{n_{cl}^{pol}}{n_{cl}^{pol}+n_{nc}^{pol}} \tag{6}$$

, in the long wavelength region. The saturated value of zonal flow is called the "residual zonal flow".

The formation of residual zonal flow is associated with the neoclassical polarization shielding effect. The inhomogeneity of the magnetic field leads to drifts of the guiding-center of ions and electrons. Because of tokamak magnetic geometry in which amplitude is proportional to $1/R$, particles in low-field-region have a small parallel velocity and undergo a magnetic mirror reflection when they move into the high-field-region. In the absence of collision, the particles reflecting on the turning point moves to the opposite direction and constructs a trapped orbit, leading to the additional polarization. As the dielectric function is increased due to neoclassical polarization density[13], time response of zonal flow is enhanced after few bounce periods.

The zonal flow consists of GAMs with a characteristic frequency (expression) and a zero frequency mode. Of these, GAMs are attenuated and disappear within a short time due to ion Landau damping, and only the zero frequency mode survives after a few bounce period. This is consistent with the residual zonal flow shown by Rosenbluth and Hinton's results. Fig.3[14] is the simulation result of the time transit behavior of the initial zonal flow. In the few bounce period $\sim 1/\omega_b$, the GAM component in the zonal flow rapidly attenuates and disappears, and it is directed to a residual zonal flow level of non-zero value. Another Fig.4[4] is the comparison between the RH expectation and flux-tube gyro-kinetic simulation result. It is shown that the RH calculation is quite valid

in this context. Not only these, many results of the simulation studies indicates that the concept of residual zonal flow is relevant in the toroidal plasma.

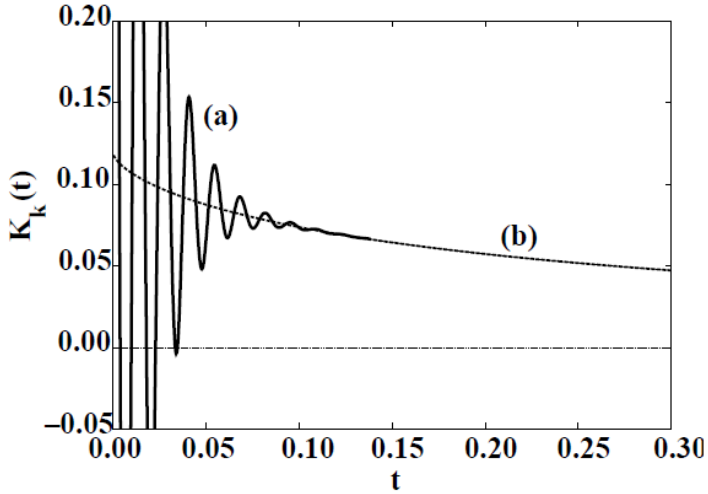

Figure 3: the decay of zonal flow.

2.3 Gyro-kinetic formalism

In this section, we introduce the gyro-kinetic formalism, the physical methodology to describe the nonlinear Vlasov system. First of all, we demonstrate the background concept of gyro-kinetic theory with a brief historical flow in section [sec]. Then we introduce two types of gyro-kinetic formalism, conventional gyro-kinetic formalism and modern gyro-kinetic formalism in section [sec] and [sec].

2.3.1 basic concept of gyro-kinetics

The development of gyro-kinetic theory was raised from the fact that plasma shows very complex dynamics over long time scales compared to the gyro-motion time scale. Before the gyro-kinetics, guiding-center theory was used to solve the

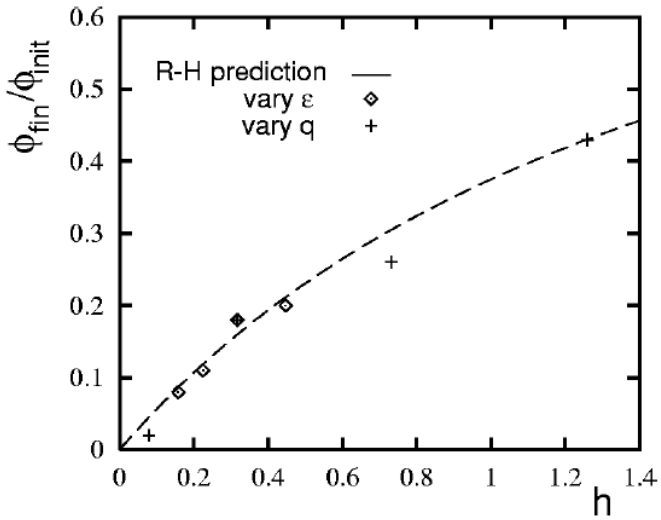

Figure 4: the decay of zonal flow.

nonlinear Vlasov kinetic equation to describe the plasma behavior. However, since there are low frequency field noises inside the turbulent plasma, it can destroys the invariance of magnetic moment of guiding-center theory. Fortunately, Hastie, Taylor, and Haas[12] showed that a new magnetic moment can be constructed as an expansion of original magnetic moment in powers of the amplitude of the perturbed field. This indicates that a new kinetic theory gyro-kinetic theory could replace the role of guiding-center theory with some relevant transformation. By using the low frequency gyro-kinetic theory, many crucial subjects were studied, especially the plasma microturbulence and its associated transport in magnetized plasma.

The goal of gyro-kinetics is to solve the self-consistent nonlinear Vlasov-Poisson system in the unhomogeneous magnetic field. In this kind of plasma, the temporal scales of electrostatic or electromagnetic fluctuation of interest are much longer than a period of cyclotron motion of a charged particle (i.e. gyro-motion). Within the framework of this system, the significance of the gyro-motion is very

weak and it is possible to construct a reduced version of kinetic equations which are focused on the phenomena of interest.

Physical characteristics of the typical fluctuation is found from experimental observations and well arranged in the reference [7]. In the typical tokamak operating condition (temperature $T = 10keV$ and magnetic field $B = 5T$ with a typical gradient length scale $L \sim 1m$), its characteristic mean frequency is on the order of the diamagnetic frequency $\omega_* \equiv k \cdot V_D$, where $V_D \equiv (cT/eB)\,\hat{b} \cdot \nabla \ln P$ is the diamagnetic drift velocity. This is the reason for naming tokamak micro-turbulence as "drift wave turbulence". The typical wavelength in perpendicular direction is on the order of several ion thermal gyro-radii $\rho_i \sim 0.2cm$ and the wavelength in equilibrium B field direction (i.e. parallel direction) is much longer than the perpendicular wavelength but much less than the equilibrium length scale. The relative amplitude of density fluctuation $\delta n/n_0$ is measured under 1% at the core and to the order of 10% at the edge. From these spatiotemporal scales of tokamak micro-turbulence, one can construct the ordering between each scale parameters, the gyro-kinetic ordering. For instance, the ratio between spatial scales is described in terms of two smallness parameters ϵ_B, ϵ_F,

$$\epsilon_B \equiv \rho_i/L_B \ll 1, \epsilon_F \equiv \rho_i/L_F \ll 1 \tag{7}$$

where L_B, L_F is the length scale of background magnetic nonuniformity and background plasma density and temperature gradient. Likewise, the temporal scale is also expressed in terms of the ordering parameter ϵ_ω,

$$\epsilon_\omega \equiv |\frac{1}{\Omega}\frac{\partial \ln \delta f}{\partial t}| \sim \frac{\omega}{\Omega} \ll 1. \tag{8}$$

The relative amplitude between equilibrium field and the fluctuating field is described in terms of the ordering parameter ϵ_δ,

$$\epsilon_\delta \equiv |\frac{\delta f}{F_0}| \sim \frac{\delta n}{n_0} \sim \frac{|\delta B|}{B_0} \ll 1. \tag{9}$$

Last, the wavelength scale of micro-turbulence is shown for each parallel and perpendicular direction,

$$|k_\perp|\rho_i \equiv \epsilon_\perp 1, |\frac{k_\perp}{k_\parallel}| \sim \frac{\omega/\Omega}{|k_\perp \rho_i|} \sim \frac{\epsilon_\omega}{\epsilon_\perp} \tag{10}$$

Note that the micro-turbulence of the high temperature tokamak plasma shows the highest linear growth at $\epsilon_\perp \sim 1$, and is nonlinearly saturated around $\epsilon_\perp \sim 0.1, 0.2$.

2.3.2 conventional gyro-kinetic formalism

In the beginning, the approach to convert guiding-center formalism to gyro-kinetic formalism was done using conventional perturbative method. Frieman and Chen[7] were the first to demonstrate the nonlinear gyro-kinetic formalism based on the multiple scale ordering expansion involving a single ordering parameter ϵ. Their effort is considered as an initiation to analytic application of gyro-kinetic theory and many nonlinear kinetic theories are based on the Frieman-Chen gyro-kinetic equations. Here, we follow the derivation of Frieman-Chen version of conventional gyro-kinetic equation as an example. Here, they use the simple gyro-kinetic ordering $\epsilon_B \sim \epsilon_F \sim \epsilon_\delta \sim \epsilon_\omega \sim \epsilon \ll 1, \epsilon_\perp \sim 1$ for microscopic fluctuations. First step of their work starts from the Vlasov kinetic equation,

$$\left(\partial/\partial t + \frac{dx}{dt}\frac{\partial}{\partial x} + \frac{dv}{dt}\frac{\partial}{\partial v}\right) F\left(x, v; t\right) = 0. \tag{11}$$

where x, v denote the position and velocity vector in particle phase-space coordinates $z = (x, v)$ and $F(x, v; t)$ denotes the particle distribution in Vlasov system. From the original statement of Vlasov equation, particle distribution is constant along an exact orbit of a single particle determined by the equations of motion.

Next step is the decomposition of the equation on the order of ϵ. During this procedure, particle distribution and the particle's equations of motion are again presented as,

$$F = F_0 + \epsilon_\delta \delta f, \qquad dz/dt = dz_0/dt + d\delta z/dt \tag{12}$$

where $(F_0, dz_0/dt)$ represent the background plasma dynamics and $(\delta f, d\delta z/dt)$ denote the perturbed plasma dynamics associated with the presence of fluctuating field perturbation $\delta E = -\nabla\delta\phi - c^{-1}\partial\delta A/\partial t$ and $\delta B = \nabla \times \delta A$. After the decomposition, Frieman and Chen introduce the spatial averaging on the decomposed version of Vlasov equation to clarify the dynamics of both large scale and small scale. With the definition $\overline{F} \equiv F_0$ and $\overline{(dz/dt)} \equiv dz_0/dt$, the averaged version of Vlasov equation yields to two equations. One is for the background plasma dynamics,

$$\left(\frac{\partial}{\partial t} + \frac{dz_0}{dt} \cdot \frac{\partial}{\partial z}\right) F_0 = -\epsilon^2 \left(\overline{\frac{d\delta z}{dt} \cdot \frac{\partial \delta f}{\partial z}}\right) \tag{13}$$

and the other is for the perturbed plasma dynamics,

$$\left(\frac{\partial}{\partial t} + \frac{dz_0}{dt} \cdot \frac{\partial}{\partial z}\right) \delta f = -\epsilon \frac{d\delta z}{dt} \cdot \frac{\partial F_0}{\partial z} - \epsilon^2 \frac{d\delta z}{dt} \cdot \frac{\partial \delta f}{\partial t} + \epsilon^2 \left(\overline{\frac{d\delta z}{dt} \cdot \frac{\partial \delta f}{\partial z}}\right). \tag{14}$$

Each equation describes the time evolution of the background plasma and perturbed plasma within the influence of fluctuating fields. Here, since the spatio-

temporal scales of two equations are very different and one can solve this two equations independently.

Here, we only focus on the fluctuating Vlasov equation of our interest. The fluctuating distribution is once more decomposed to the adiabatic part and the non-adiabatic part. Adiabatic response is fast and direct response of field perturbation. Including this, the fluctuating distribution is described as,

$$\delta f = \frac{q}{m}\left[\delta\phi\frac{\partial}{\partial} + \left(\delta\phi - \frac{v_\parallel}{c}\delta A_\parallel\right)\frac{\partial}{B\partial\mu}\right]F_0 + \delta g. \tag{15}$$

The non-adiabatic component is again decomposed of the gyro-phase-independent part which is in out interest and gyro-phase-dependent part. Here, the decomposition is established in the gyro-averaging process of fluctuating Vlasov equation. Note that the gyro-averaging $\langle ... \rangle \equiv (1/2\pi)\int_0^\infty (...)$ leads the equation to represent the dynamics of guiding-center. Expanding $\delta g = \delta g_0 + \delta g_1 + ...$ which $\partial\delta g_0/\partial\alpha = 0$, one can obtain the guding-center kinetic equation,

$$\left(\frac{\partial}{\partial t} + \frac{d\langle z_0\rangle}{dt}\cdot\frac{\partial}{\partial z}\right)\delta g_0 = \langle(...)\rangle \tag{16}$$

with

$$\delta g_0 = -\frac{q}{m}\langle\delta\psi\langle\delta A\rangle\frac{\partial F_0}{B\partial\mu} + \delta h. \tag{17}$$

where $\delta\psi$ is field potential $\delta\psi = \delta\phi - \frac{v_\parallel}{c}\delta A_\parallel$. By substituting the non-adiabatic component δg into the fluctuating Vlasov equation 14, the nonlinear kinetic equation for the gyro-phase-independent non-adiabatic part is obtained,

$$\left(\frac{\partial}{\partial t} + v_\parallel\nabla_\parallel + v_D\cdot\nabla\right)\delta h = -\left(q\frac{\partial\langle\delta\psi\rangle}{\partial t}\frac{\partial}{\partial} + \frac{c\hat{b}}{B}\times\nabla\langle\delta\psi_g c\rangle\cdot\nabla\right)F_0 - \frac{c\hat{b}}{B}\times\nabla\langle\delta\psi_g c\rangle\cdot\nabla\delta h \tag{18}$$

The Vlasov kinetic equation for non-adiabatic part δh includes up to the order $O(\epsilon^2)$ and thus represents the nonlinear coupling terms such like the fluctuating

ExB nonlinearity $\sim \left(c\hat{b}/B\right) \times \nabla\langle\delta\phi\rangle$.

Despite their pioneering work, their equations are valid up to order ϵ^2 and do not satisfy the conservation law such as energy or phase space volume. A lack of these kind of conserved quantities can induce the fictitious quantities in the long time behavior of the Hamiltonian system.

2.3.3 modern gyro-kinetic formalism

In contrast to the conventional gyro-kinetic theory which is based on the perturbative expansion in power of smallness parameter and gyrophase averaging, the modern gyro-kinetic theory is based on the phase-space coordinate transformation to reduce the dependency of inconsiderable variable. A key point of derivation of the modern gyro-kinetic equations is that the original particle Lagrangian system is transformed to a new gyro-center phase space Lagrangian system. By doing so, the equations of motion in gyro-center coordinates are separated from the fast gyro-motion time scale at arbitrary orders in ϵ. Following this nonlinear kinetic theory, one can observe the plasma dynamics of our interest in the slow time scale. Also, the important underlying conservation laws of the original Hamiltonian system are kept during the transformation. The modern gyro-kinetic theory guarantees the correctness of physical quantities in various expansion ordering.

Many significant works of the transformation from guiding-center coordinates (which is exact same as the original particle coordinates) to gyro-center coordinates were performed by Littlejohn in early 80's. His pioneering works mainly explain the Lie transformation perturbation theory as a tool for perturbation transformation in the non-canonical coordinates. The significance of the Lie transformation is that it replaces the complex transformation based on mixed variable generating functions used in the conventional gyro-kinetic formalism.

It is very simple and powerful mathematical approach for perturbation transformation, which guarantees the strong accuracy even in the higher order of ϵ. On here, we briefly explain the Lie transformation and use it to derive the modern gyro-kinetic formalism. Details of the demonstration is illustrated in [16].
One can assume a system that the coordinates $\{x^i\}$ is related to a perturbative vector field $\{X^i\}$ satisfying

$$\frac{dx^i}{dt} = X^i(x) = \sum_{k=0}^{\infty} \epsilon^k X_k^i(x), \tag{19}$$

where ϵ is an ordering parameter. To simplify the equations of motion, one can find a new coordinates system $\bar{x}^i = x^i + O(\epsilon)$, which is the identity at the 0-th order. Then the transformation T from $\{x^i\}$ to $\{\bar{x}^i\}$ is defined in terms of ϵ, i.e. $\bar{x} = T(x;\epsilon)x$. Now, let us consider one more vector field G, which is associated with the original coordinates x^i

$$\frac{dx^i}{d\epsilon} = G^i(x). \tag{20}$$

Since this coordinate transformation is near-identity infinitesimal transformation, T is expressed with the generating vector field G, $T(x;\epsilon) = exp\left(\epsilon G(x)\right)$. In the same time, vector field X is also changed to a new vector field $\bar{X}$ by the tangent mapping T_*, $\bar{X} = T_* X$. Here, we introduce the Lie derivative L_G which is defined as,

$$L_G X = \lim_{\epsilon \to 0} \frac{1}{\epsilon} \left(X - \bar{X} \right), \tag{21}$$

in which X and $\bar{X}$ is presented at the same point, i.e. $x = T^{-}1\bar{x}$. The Lie derivative is in general the Lie bracket or commutator of two vector fields,

$$L_G X = [G, X] \tag{22}$$

Using the analogy of infinitesimal transformation, we have $T_* = exp\,(-\epsilon L_G)$. Thus, both coordinate transformation and tangent mapping can be written as a power series related to the ordering parameter ϵ and generator G. Meanwhile, it is obvious that the pull-back mapping T^* can be also described in terms of the Lie derivative L_G, $T^* = exp\,(+\epsilon L_G)$.

This is only one case of transformation desirable for the $O(\epsilon)$ term with a single generator. To generalize this, one can introduce a sequence of generator $G_1, G_2, ...$, transformation operators $T_1, T_2, ...$, defined as,

$$T_n = exp\,(\epsilon^n G_n)\,, \tag{23}$$

and the corresponding mapping with n-th order Lie derivative L_n,

$$T_{*n} = exp\,(-\epsilon^n L_n) \qquad T_n^* = exp\,(+\epsilon^n L_n)\,. \tag{24}$$

By integrating whole order of the operator, the overall transformation operator T is expressed as,

$$T = ...T_3 T_2 T_1 \quad T_* = ...T_{*3} T_{*2} T_{*1} \quad T^* = ...T_3^* T_2^* T_1^*. \tag{25}$$

Using the Lie transformation, it is possible to convert the perturbed gyro-phase dependent Hamiltonian system to the perturbed gyro-phase independent Hamiltonian system with a new fascinating coordinate called "gyro-center coordinates". Following the Hahm's transformation[10], the particle phase-space Lagrangian γ is described as,

$$\gamma = \left(\frac{e}{c}A + mv\right) \cdot dx - \left(\frac{1}{2}mv^2 + e\delta\phi\right) dt \tag{26}$$

where A is vector potential for equilibrium magnetic field B, $v_\parallel$ is parallel velocity, μ is magnetic moment of charged particle, $\Omega = \frac{eB}{mc}$ is gyro-frequency and $\hat{b} = \frac{B}{|B|}$. Here, $e\delta\phi$ denotes a small-scale wavelength field fluctuation. One can firstly perform a guiding-center phase-space transformation which reduces the gyro-phase dependence to obtain the unperturbed (i.e. without electrostatic fluctuation) guiding-center phase-space Lagrangian,

$$\gamma_{gc} = \left(\frac{e}{c}A + mv_\parallel \hat{b}\right) \cdot dR + \frac{\mu B}{\Omega} d\Theta - \left(\frac{1}{2}mv_\parallel^2 + \mu B\right) dt. \tag{27}$$

When the small electrostatic fluctuation $\delta\phi$ is introduced on the system, the guiding-center of particle is affected by fluctuation induced motion. Thus, the perturbed Lagrangian,

$$\delta\gamma = -e\delta\phi(R + \rho)dt, \tag{28}$$

is considered as 1st order Hamiltonian. By definition, the Lie-transformed Lagrangian is expressed as

$$\bar{\gamma} = T^{-1}\gamma + dS \tag{29}$$

where $\bar{\gamma} = \bar{\gamma}_\mu d\bar{Z}^\mu$ and S represents a gauge transformation in phase space. This is expanded on the powers of ϵ as follows :

$$\bar{\gamma}_0 = \gamma_0 + dS_0, \tag{30}$$

$$\bar{\gamma}_1 = \gamma_1 - L_1\gamma_0 + dS_1, \tag{31}$$

$$\bar{\gamma}_2 = \gamma_2 - L_1\gamma_1 + \left(\frac{1}{2}L_1^2 - L_2\right)\gamma_0 + dS_2. \tag{32}$$

where $\partial z^\mu/\partial\epsilon^n = g_n^\mu(z)$ and $(L_l\gamma_n)_\mu = g_l^\nu\left(\frac{\partial\gamma_{n\mu}}{\partial z^\nu} - \frac{\partial\gamma_{n\nu}}{\partial z^\mu}\right)$. Here, one can choose the generating function g and the gauge transformation dS so that every gyro-phase dependence is absorbed in the generating function during the calculation.

By doing so, one can get the gyro-phase independent Hamiltonian $\bar{\gamma}_t$ order by order. The well-organized results are introduced in [10],

$$\bar{\gamma}_{1t} = -e\langle\delta\phi\rangle_g, \tag{33}$$

$$\bar{\gamma}_{2t} = \frac{e^2}{2\Omega}\left(\frac{\partial}{\partial\mu}\langle\widetilde{\delta\phi}\rangle_g + \frac{1}{\Omega}\langle\nabla\widetilde{\delta\Phi}\cdot\hat{b}\times\nabla\widetilde{\delta\phi}\rangle_g\right), \tag{34}$$

with proper generating functions. Note that

$$\langle\delta\phi\rangle = \frac{1}{2\pi}\oint d\alpha\phi(R+\rho,t), \quad \widetilde{\delta\phi} = \delta\phi - \langle\delta\phi\rangle_g, \tag{35}$$

and

$$\widetilde{\delta\Phi} = \int^{\alpha}\widetilde{\delta\phi}d\alpha. \tag{36}$$

Substituting the Hamiltonian into the guiding-center Lagrangian, it is transformed to the gyro-center Lagrangian with the presence of electrostatic field fluctuation,

$$\bar{\gamma}_{gy} = \left(\frac{e}{c}\bar{A} + m\bar{v}_{\parallel}\hat{b}\right)\cdot d\bar{R} - \left(\frac{1}{2}m\bar{v}_{\parallel}{}^2 + \bar{\mu}B + e\delta\Phi\right)dt \tag{37}$$

where $\delta\Phi$ is effective potential,

$$\delta\Phi = \langle\delta\phi\rangle_g - \frac{e^2}{2\Omega}\left(\frac{\partial}{\partial\overline{\mu}}\langle\delta\tilde{\phi}^2\rangle_g + \frac{1}{\Omega}\langle\nabla\widetilde{\delta\Phi}\cdot\hat{b}\times\nabla\widetilde{\delta\phi}\rangle_g\right) \tag{38}$$

From this, note that Hamiltonian system is preserved from the original particle coordinates so that energy in the system is automatically conserved. Also, using the Euler-Lagrange equations, the gyro-averaged motion of single particle is demonstrated clearly and precisely. The gyro-kinetic Vlasov equation is now described without the dependency of gyro-phase,

$$\left(\frac{\partial}{\partial t}+\frac{d\bar{R}}{dt}\cdot\nabla_{\bar{R}}+\frac{d\bar{v_{\parallel}}}{dt}\frac{\partial}{\partial\bar{v_{\parallel}}}\right)\bar{F}\left(\bar{R},\bar{v_{\parallel}},\bar{mu}\right)=0. \tag{39}$$

2.4 Slowing down distribution

In general, tokamak plasma is considered as a quasi-steady state, which means that the thermodynamic state of plasma is near the equilibrium and the slow change arises from the nonlinear interactions of the fluctuating perturbation. Here, the choice of the equilibrium is naturally the Maxwellian equilibrium. However, when it comes to the fusion plasmas, it is needed to take account of the energetic ions (such as fusion alpha ions) passing through the plasma. The kinetic energy of energetic ions is typically much larger than the temperature of the background plasma. In terms of this, one should consider a new equilibrium driven by the interaction between background plasma and energetic ions.

When highly energetic particles are injected into the plasma, they are colliding with the background plasma particles many times and thus thermalize to the dynamic equilibrium. The velocity of energetic particle is assumed to be much less than thermal velocity of background electron, but much greater than thermal velocity of background ions, i.e. $v_{Ti} \ll V_0 \ll v_{Te}$. The frictions between energetic particles and background plasmas can be considered as two types, one the particle-ion collision and the other the particle-electron collision. In this section, we briefly demonstrate this two types of collision.

2.4.1 particle-electron collision

Particle-electron collision can be considered as the collision between massive, stationary ions and electrons in the view of the co-moving frame of energetic particle. Typically, It is easy to trasnfer the momentum to the energetic particle,

but not the energy. Thus, the velocity vector of energetic is deflected in the laboratory frame and the energy this perpendicular motion is on the order of (m_e/M_p), where M_p is the mass of energetic particle. This is the typical case of small angle scattering of electrons with ions, and the solution of this is well demonstrated in the [9]. Assuming that background plasma is in the Maxwellian equilibrium the slowing down process is described with the averaged collision frequency ν_{eP},

$$\frac{d}{dt} < V >= -\frac{\sqrt{2} n_e Z_P^2 e^4 m_e^{1/2} \ln \Lambda}{12\pi^{3/2} \epsilon_0^2 M_P^2 T_e^{3/2}} VV \tag{40}$$

where n_e, m_e, T_e are electron quantities; density, mass, and temperature, respectively, Z_P is charge number of particle, and $\ln \Lambda$ is the effective scattering parameter. Note that the characteristic time scale for particle-electron collisions only depends on the electron-based parameters such as electron density and the 3/2 power of the electron temperature. By taking the velocity moment in equation 40, we obtain an expression for the evolution of kinetic energy of particle,

$$\frac{d}{dt} W_P = -\frac{\sqrt{2} n_e Z_P^2 e^4 m_e^{1/2} \ln \Lambda}{12\pi^{3/2} \epsilon_0^2 M_P^2 T_e^{3/2}} W_P \tag{41}$$

2.4.2 particle-ion collision

Next let us consider the collisions of energetic particles with background plasma ions. In general, the mass of energetic particle is larger than that of background ions, but not as much as the electron collision case. Indeed, two masses have a comparable order of magnitude. It means that when colliding to each other energy transfer from energetic particle to background ions is dominant same as the momentum transfer. In the laboratory frame, energetic particles take a role of injected beam particle and this is regarded as the ion-ion . Like the electron collision case, the slowing down process due to particle-ion

collision is described as,

$$\frac{d}{dt} < V >= -\frac{n_i Z_P^2 e^4 m_e^{1/2} \ln \Lambda}{4\pi\epsilon_0^2 M_i M_P V^3} V \tag{42}$$

where n_i, M_i is ion density and ion mass. Note that the relative velocity $|v - V|$ is approximated to V, since the energetic particle velocity exceeds the thermal ion velocity (i.e. $v_T i \ll V_P$. By taking the velocity moment in equation 42, When high energy particles are injected in the plasmas, we can use the slowing down distribution as an equilibrium distribution function, we obtain,

$$\frac{d}{dt} W_P = -\frac{\sqrt{2} n_i Z_P^2 e^4 M_i^{1/2} \ln \Lambda}{8\pi^{3/2}\epsilon_0^2 M_i W_P 1/2} \tag{43}$$

2.4.3 critical energy

If we combine two expressions of evolution of the particle energy for ion collision and electron collision, we obtain

$$\frac{d}{dt} W_P = -\frac{\sqrt{2} n_e Z_P^2 e^4 m_e^{1/2} \ln \Lambda}{6\pi^{3/2}\epsilon_0^2 M_P} \left(\frac{W_P}{T_e^{3/2}} + \frac{C}{W_P^{1/2}} \right) \tag{44}$$

where

$$C = \frac{3\sqrt{pi} M_P^{3/2}}{4 m_e^{1/2} M_i} \tag{45}$$

Considering the significance of each collision-induced energy transfer term, the critical energy of particle is given by

$$W_{crit} = C^{2/3} T_e \tag{46}$$

It means that as the particle energy is larger than the critical energy ($W_P W_{crit}$), then the particle-electron collision is much dominant than the particle-ion collision in terms of the slowing down process.

2.4.4 slowing down equilibrium

The dynamical evolution of slowing down process due to the collision with background ions and electrons can be expressed using the Fokker-Planck equation. Assuming that the source of energetic particle is isotropic, we can neglect the effect of pitch-angle scattering during the collision. Thus, we can also neglect the velocity diffusion term in the general Fokker-Planck equation, and only consider the dynamic friction due to the background plasmas. It is written as,

$$\left(\frac{\partial f}{\partial t}\right)_{coll} = -\nabla_V \cdot \left(\frac{d < V >}{dt} f\right). \tag{47}$$

Substituting our previous expressions in this equation, we obtain

$$\left(\frac{\partial F_P}{\partial t}\right) = -\frac{n_e Z_P^2 e^4 \ln \Lambda}{4\pi\epsilon_0^2 M_P M_i} \nabla_V \cdot \left[\frac{V}{V^3}\left(1 + \frac{V^3}{V_c^3}\right) F_P\right] \tag{48}$$

where $V_c = \left(\frac{2W_crit}{M_P}\right)^{1/2}$ is the critical velocity. Since we are assuming the isotropic system, the direction of particle velocity is not our concern and the equation is simplified as

$$\left(\frac{\partial F_P}{\partial t}\right) = -\frac{n_e Z_P^2 e^4 \ln \Lambda}{4\pi\epsilon_0^2 M_P M_i} \frac{1}{V^2} \frac{\partial}{\partial V} \left[\left(1 + \frac{V^3}{V_c^3}\right) F_P\right]. \tag{49}$$

This dynamic friction term is balanced with the source term. Specifically, we assume the isotropic source with constant production rate. Then the source term is given as

$$\left(\frac{\partial F_P}{\partial t}\right)_{source} = \frac{S\delta\left(V - V_0\right)}{4\pi V^2}. \tag{50}$$

Adding this term into the equation 49, the source term will balance with the friction term and finally goes to the dynamic equilibrium over long time. From this, the steady-state distribution function is obtained in the assumption $\frac{\partial}{\partial t} - >$

0,

$$0 = -\frac{n_e Z_P^2 e^4 \ln\Lambda}{4\pi\epsilon_0^2 M_P M_i}\frac{1}{V^2}\frac{\partial}{\partial V}\left[\left(1+\frac{V^3}{V_c^3}\right)F_P\right] + \frac{S\delta\left(V-V_0\right)}{4\pi V^2} \tag{51}$$

By integrating in the velocity space, This gives a solution,

$$F_{SD}(v) = \frac{n_P}{4\pi v_c^3 I_2}\frac{H(V_0-V)}{1+(\frac{V}{V_c})^3} \tag{52}$$

where V_0 is an initial beam velocity, V_c is slowing down critical velocity,

$$V_c^3 = 3\sqrt{\frac{\pi}{2}}\frac{m_e}{m_\alpha}Z_{eff}\left(\frac{T_e}{m_e}\right)^{3/2} \tag{53}$$

and $I_n = \int_0^{v_\alpha/v_c}\frac{x^n}{1+x^3}dx$. For a proper normalization, we define the effective temperature of slowing down distribution by the quadratic moment of velocity,

$$\int v^2 F_{SD}(v)d^3v = \int v^2 F_{Max}(v)d^3v\frac{T_{Max}}{T_{SD}} = \frac{I_4}{3I_2} \tag{54}$$

3 Precedent Study

Previous studies on residual zonal flow mainly focused on accurate calculation and implementation of residual zonal flow. Rosenbluth and Hinton[17] demonstrated the existence of residual zonal flow in ITG turbulence in tokamak by solving a nonlinear gyro-kinetic equation through a conventional approach. Their analytical solution also showed that the residual zonal flow is related to neoclassical polarization shielding due to bounce orbit, and it is calculated to have the same approximation as in (expression) in the long wavelength region. Later, Hinton and Rosenbluth[14] extended their study to the collisional realm. The effect of plasma shaping on residual zonal flow was investigated. Xiao and Catto[21] express the dependency of residual zonal flow according to plasma shaping parameters as an analytical expression. Despite their excellent

research, their research has shown that the radial wavelength is close to the long wavelength region longer than the ion poloidal gyro-radius.

Attempts have been made to obtain residual zonal flow for short wavelength regions. Jenko et al. [15] showed that the gyro-kinetic simulation shows that the residual zonal flow level increases over short wavelengths in the electron temperature gradient (ETG) turbulence. Xiao and Catto[22] performed the theoretical studies on neoclassical polarization shielding at short wavelengths. Following the Rosenbluth and Hinton's methodology, they calculated the residual zonal flow for various phases of short wavelength regime analytically and numerically. The limitation of their work was that they only considered the finite orbit width (FOW) effect when calculating the neoclassical polarization. The Larmor radius (FLR) effect is also included in the neoclassical polarization.

Many of the calculations of residual zonal flow using modern gyro-kinetic theory have also been done. Wang and Hahm[20] analytically determined residual zonal flow for arbitrary wavelengths using modern gyro-kinetic formalism. Their calculations took into account both the FLR effect and the FOW effect on the neoclassical polarization, and calculated the residual zonal flow for the wavelength regime including ITG turbulence and ETG turbulence. Duthoit and Brizard, Hahm[5] elaborated the classical and neoclassical polarization densities while showing the analytic expression of the bounce / transit orbit in the tokamak geometry. However, the expression is too complex and the FLR effect is neglected when calculating the neoclassical polarization.

All of the residual zonal flow studies described above use the Maxwellian distribution function as the equilibrium distribution function. No studies have yet been conducted using other equilibrium distribution functions. The contribution of the equilibrium distribution to the zonal flow is unrevealed, but considering the plasma plasmas in the future tokamak devices such as ITER

or DEMO it is necessary to study the residual zonal flow in the circumstance of burning plasma. In this paper, we focused on the effect of slowing down distribution function on each classical and neoclassical polarization using the modern gyro-kinetic formalism. During this, FLR effect and FOW effect are sufficiently covered in the calculation. The result includes not only the comparison between the slowing down case and equivalent Maxwellian case but also the residual zonal flow dependent of the initial energy of energetic ions.

4 Residual Zonal Flow for Slowing Down Distribution Function

In this section, we demonstrate how the polarization density is calculated using modern gyro-kinetic theory. Firstly, we describe the analytic formula of each polarization density by using pull-back transformation of modern gyro-kinetic formalism. The expression is calculated for the slowing down equilibrium distribution function. Each polarization density is compared to that for the equivalent Maxwellian case. Finally, residual zonal flow level for slowing down distribution function is described as a combination of classical and neoclassical polarization density. The dependency of the initial particle energy is also presented.

4.1 Analytic expression of polarization density

In the section 2.3 and 2.4, we introduced the modern gyro-kinetic formalism and the slowing down distribution briefly. Here, we derive expressions for the classical/neoclassical polarization density by pull-back transforming the charge density from the gyro-center/bounce gyro-center phase space to the particle phase space, respectively. Details can be found from the following papers. Wang and Hahm[20] presented the generalized expressions for both classical and

neoclassical polarization density using the modern gyro-kinetics and bounce gyrokinetics. By doing so, they fully consider the FLR effect and FOW effect in the expression. Duthoit, Brizard, and Hahm[5] improved the analytic approximations for trapped and passing orbit to calculate the neoclassical polarization density more accurately. Since their analytic expression is too complex for our purpose in this paper, we follow the Wang-Hahms method when calculating the classical and neoclassical polarization density using the pull-back transform. In this way, both classical and neoclassical polarization density are derived physically and systematically. The schematic description of pull-back transformations is illustrated explicitly in Fig. 2 of reference [20].

Now we present the particle charge density in the gyrokinetic Poisson equation. This is expressed in terms of the distribution in the gyro-center phase space, and in the bounce gyro-center phase space. In this procedure, two consecutive pull-back transformations are performed, one from gyro-center to particle phase space and the other from bounce gyro-center to particle phase space. Each pull-back transformation results in two different polarization densities, the classical polarization density from the gyro-center transformation and the neoclassical polarization density from the bounce gyro-center transformation.

Starting from the particle phase space, the charge density for each species s appears in the Poisson equation as below.

$$\begin{aligned}
\nabla^2\phi(x,t) &= 4\pi\sum_s q_s n_s(x) = 4\pi\sum_s q_s\int d^3v f_s(x,v,t) \qquad (55)\\
&= 4\pi\sum_s q_s\int d^3R dv_\parallel d\mu F_{gc,s}(R,v_\parallel,\mu,t)\delta(R+\rho-x)\\
&= 4\pi\sum_s q_s\int d^6Z F_{gc,s}(Z)\delta(R+\rho-x)
\end{aligned}$$

Here, note that $f_s(x;v;t) = F_{gc,s}(Z)$. Via inverse-transform of the kernel in density expressions to gyro-center phase space, the guiding-center phase space

distribution function gets Lie transformed to the gyro-center phase space distribution function with the generator of inverse Lie transformation $T_g y^{-1}$. Then the particle density function can be written in terms of the distribution in the gyro-center phase space,

$$\begin{aligned} n(x,t) &= \int d^6\bar{Z}\left(T_{gy}^{-1}F_{gy}(\bar{Z})\right)\delta(T_{gc}^{-1}R-x) \\ &\simeq \int d^6\bar{Z}\left(F_{gy}(\bar{Z})+G_1^{\bar{\mu}}\frac{\partial}{\partial\bar{\mu}}F_{gy}(\bar{Z})\right)\delta(T_{gc}^{-1}R-x) \\ &= n_{gy}(x,t)+n_{cl}(x,t) \end{aligned} \tag{56}$$

with

$$n_{gy}(x,t)=\int d^6\bar{Z}F_{gy}(\bar{Z})\delta(T_{gc}^{-1}R-x) \tag{57}$$

$$n_{cl}(x,t)=\int d^6\bar{Z}G_1^{\bar{\mu}}\frac{\partial}{\partial\bar{\mu}}F_{gy}(\bar{Z})\delta(T_{gc}^{-1}R-x) \tag{58}$$

where the first term is the gyro-center density (denoted by n_{gy}) and the last term is the classical polarization density (denoted by n_{cl}), the difference between the particle charge density and the gyro-center density. Note that we only consider the 1st order contribution of the generator of inverse Lie transformation, especially the magnetic moment part $G_1^{\bar{\mu}}$ compared to the $G_1^{\bar{\mu}}$ term. Other moment contribution $G_1^{\bar{R}}, G_1^{\bar{v}_\parallel}$ are of higher order in the spatial ordering[].

Next, the gyro-center density can be also written in terms of the distribution in the bounce gyro-center phase space. Using the fact that guiding-center phase corresponds to the lowest order gyro-center phase space in the gyro-kinetic ordering, one can use an identity that $F_{gy}(\bar{Z})=F_{bgc}(Z_{bgc})$. Then the gyro-center density function can be written in terms of the distrbution in the bounce gyro-center phase space,

$$n_{gy}(x,t) = \int d^6 Z_{bgc}F_{bgc}\left(Z_{bgc}\right)\delta\left(T_{gc}^{-1}T_{bgc}^{-1}R_{bgc}-x\right) \tag{59}$$

$$
\begin{aligned}
&= \int d^6\hat{Z}\left(T_{bgy}^{-1}\hat{F}\left(\hat{Z}\right)\right)\delta\left(T_{gc}^{-1}T_{bgc}^{-1}R_{bgc}-x\right)\\
&\simeq \int d^6\hat{Z}\left(\hat{F}\left(\hat{Z}\right)+G_1^{\hat{J}}\frac{\partial}{\partial\hat{J}}\hat{F}\left(\hat{Z}\right)\right)\delta\left(T_{gc}^{-1}T_{bgc}^{-1}R_{bgc}-x\right)\\
&= n_{bgy}(x,t)+n_{nc}(x,t)
\end{aligned}
$$

with

$$
n_{bgy}(x,t)=\int d^6\hat{Z}\hat{F}\left(\hat{Z}\right)\delta\left(T_{gc}^{-1}T_{bgc}^{-1}R_{bgc}-x\right) \tag{60}
$$

$$
n_{nc}(x,t)=\int d^6\hat{Z}G_1^{\hat{J}}\frac{\partial}{\partial\hat{J}}\hat{F}\left(\hat{Z}\right)\delta\left(T_{gc}^{-1}T_{bgc}^{-1}R_{bgc}-x\right) \tag{61}
$$

where the first term is the bounce gyro-center density (denoted by n_{bgy}) and the last term is the neoclassical polarization density (denoted by n_{nc}), the difference between the gyro-center density and the bounce gyro-center density. As we did for the classical polarization density case, we neglect the other moment contribution $G_1^{\hat{R}}, G_1^{\hat{v}_\parallel}$, since compared to the $G_1^{\hat{J}}$ term they are of higher order in the spatial ordering [20].

With the generator of the inverse Lie transform given in reference [20], we can express each polarization density analytically. By flux-surface averaging to keep only the zonal component, we obtain,

$$
[n_{cl,k}]_\psi \simeq n_k e^{iS(\bar{\psi})}\int\left(1-|\langle e^{i\delta\zeta}\rangle_g|^2\right)\times\left(-\frac{T\partial}{B\bar{\mu}}\right)F_{SD}(\bar{Z})2\pi d\bar{v}_\parallel\frac{Bd\bar{\mu}}{m} \tag{62}
$$

$$
[n_{nc,k}]_\psi \simeq n_k e^{iS(\hat{\psi})}\int|\langle e^{i\delta\zeta}\rangle_g|^2\left(1-|\langle e^{i\Delta\zeta}\rangle_{b,t}|^2\right)\times\left(-\frac{T\partial}{\omega_{b,t}\partial\hat{J}}\right)F_{SD}(\hat{Z})\frac{d\hat{J}}{qR_0}\frac{Bd\hat{\mu}}{m} \tag{63}
$$

where $\delta\zeta = k\cdot\rho$ is the particle's excursion from the gyro-center, $[...]_\psi$ denotes the flux-surface averaging, $\Delta\zeta$ is the particle's excursion from the bounce gyro-center,

$$\Delta\zeta = k\cdot\rho_\theta \simeq \sqrt{2\epsilon}k_r\rho_{\theta i}\sqrt{\kappa} \times \begin{bmatrix} cn\left(\xi_b|\kappa\right) & for\,trapped\,particle \\ dn\left(\xi_t|\kappa^{-1}\right) & for\,passing\,particle \end{bmatrix}$$

and n_0 is initially perturbed density, $n_k = \frac{e\phi_k(0)}{T}n_0$.

In this section, we have systematically derived the classical and neoclassical polarization density. Note that this result has been obtained with the consideration of full FLR/FOW effect. Detailed calculation of each polarization density is presented in next subsections.

$$\Delta\zeta = k\cdot\rho_\theta \simeq \sqrt{2\epsilon}k_r\rho_{\theta i}\sqrt{\kappa} \times \begin{bmatrix} cn\left(\xi_b|\kappa\right) & for\,trapped\,particle \\ dn\left(\xi_t|\kappa^{-1}\right) & for\,passing\,particle \end{bmatrix} \tag{64}$$

and n_0 is initially perturbed density, $n_k = \frac{e\phi_k(0)}{T}n_0$.

4.1.1 Calculation of classical polarization density

As demonstrated before, classical polarization density is the difference between the particle density and the gyro-center density. The main reason for this is that polarization due to the gyration motion of ions and electrons changes the dielectric response of plasma. Thus, classical polarization density is sensitively affected by FLR effect. Since we consider the slowing down distribution, its velocity space composition is quite different from the equivalent Maxwellian distribution. It results in a difference of classical polarization density between slowing down case and equivalent Maxwellian case.

Because the generator term derived from the slowing down dis distribution function is too complex to solve directly, we only consider the two limiting cases, the long wavelength range $k_r\rho_\perp < 1$, and short wavelength range $k_r\rho_\perp > 1$. Then, we construct a connection formula using the method employed in Ref. [20].

With the gyro-excursion term $\left(1 - |\langle e^{i\delta\zeta}\rangle_g|^2\right)$ which has a quadratic dependency

of Bessel function $J_0(x)$, the analytic expression of classical polarization is described as,

$$
\begin{aligned}
[n_{cl,k}]_\psi &= \frac{T}{T_c} n_k e^{iS(\bar{\psi})} \int \left(1 - J_0^2\left(k_r \rho_\perp\right)\right) \left(-\frac{T\partial}{B\bar{\mu}}\right) \left(\frac{1}{4\pi v_c^3 I_2} \frac{1}{1+\left(\frac{v}{v_c}\right)^3}\right) 2\pi v^2 dv d\cos\theta \\
&= \frac{T}{T_c} n_k e^{iS(\bar{\psi})} \int \left(1 - J_0^2\left(k_r \rho_c x \sin\theta\right)\right)) \left(-\frac{1}{2I_2} \frac{3x}{\left(1+x^3\right)^2}\right) x^2 dx d\cos\theta \\
&= \frac{T}{T_c} n_k e^{iS(\bar{\psi})} \int G(x,\theta) \frac{1}{2I_2} \frac{1}{1+x^3} dx d\cos\theta \qquad (65)
\end{aligned}
$$

where function G is described as,

$$
\mathrm{G(x,}\theta) = 1 - J_0^2(t) + 2tJ_0(t)J_1(t) \approx \begin{bmatrix} \frac{3}{2}t^2 & for & |t| \ll 1 \\ 1 - \frac{2}{\pi}\cos 2t & for & |t| \gg 1 \end{bmatrix} (t = k_r \rho_c x \sin\theta)
$$

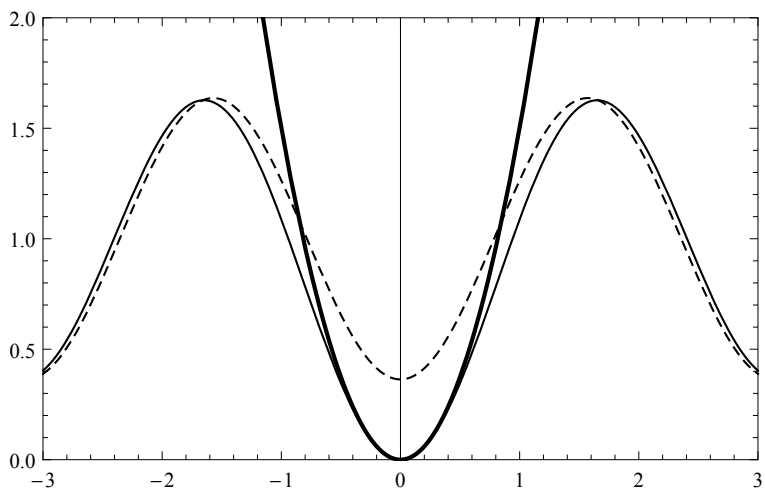

Figure 5: $G(x,\theta)$(solid) approximated in long wavelength limit(thick) and short wavelength limit(dashed)

In the long wavelength limit, the formula is simply calculated to,

$$
\begin{aligned}
[n_{cl,k}]_\psi &= \frac{T}{T_c} n_k e^{iS(\bar{\psi})} \int \frac{3}{2} x^2 \left(1 - \cos^2\theta\right) \frac{1}{2I_2} \frac{1}{1+x^3} dx d\cos\theta \\
&= \frac{T}{T_c} n_k e^{iS(\bar{\psi})} k_r^2 \rho_c^2 \left(= n_k e^{iS(\bar{\psi})} k_r^2 \rho_i^2\right), \qquad (66)
\end{aligned}
$$

so that the result is just same as the RH calculation result for Maxwellian distribution.

In the short wavelength limit, however, it is too complex to express analytically. The simplified version of the formula is,

$$\begin{aligned}[n_{cl,k}]_{\psi} &= \frac{T}{T_c} n_k e^{iS(\bar{\psi})} \int \left(1 - \frac{2}{\pi}\cos 2k_r\rho_c x \sin\theta\right) \frac{1}{2I_2} \frac{1}{1+x^3} dx d\cos\theta \\ &= \frac{T}{T_c} n_k e^{iS(\bar{\psi})} \Lambda\left(k_r\rho_c; \frac{v_0}{v_c}\right), \end{aligned} \tag{67}$$

where normalized function Λ is semi-analytic expression,

$$\Lambda\left(x; a\right) \equiv \int_0^a \frac{1 + H_{-1}(2xt)}{1+t^3} \frac{dt}{I_2}. \tag{68}$$

Here, we use the Bessel-Fourier identity with the Struve H function $H_n(x)$, $\int_{-1}^{1} \cos(2k_r\rho_c x \sin\theta) d\cos\theta = \pi H_{-1}(2k_r\rho_c x)$.

Combining each term by using simple connection formula, classical polarization density for slowing down distribution is expressed as,

$$[n_{cl,k}]_{\psi} = n_k \left\{ \frac{1}{1+k_r^2\rho_c^2} \frac{1}{k_r^2\rho_c^2} + \frac{k_r^2\rho_c^2}{1+k_r^2\rho_c^2} \frac{1}{\Lambda\left(k_r\rho_c; \frac{v_\alpha}{v_c}\right)} \right\}^{-1}. \tag{69}$$

It is shown in the Fig.6 that there's no difference between slowing down case and equivalent Maxwellian case in the long wavelength regime. However, the slowing down case gets much bigger than equivalent Maxwellian case on the range $k_r\rho_{\theta i} \simeq 1$. The interesting thing is that for each wavelength limit two results from different distribution has the same polarization value.

4.1.2 Calculation of neoclassical polarization density

Similar with the classical polarization density, neoclassical polarization density is a difference between the gyro-center density and the bounce gyro-center

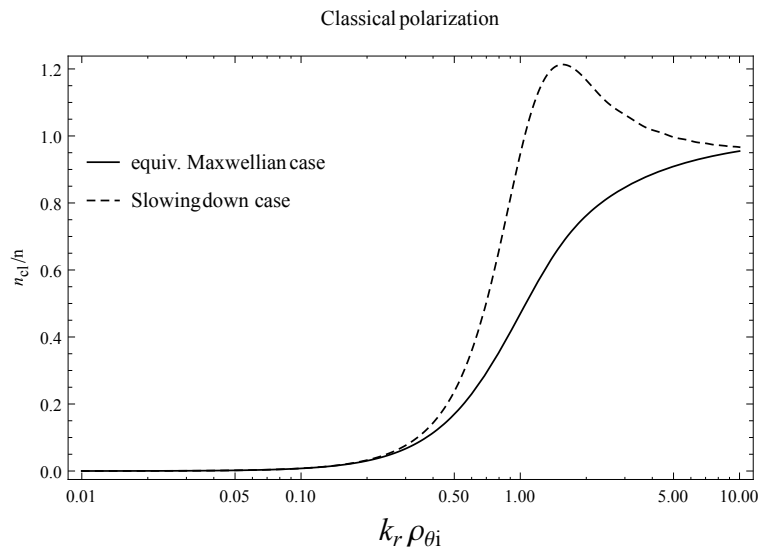

Figure 6: n_{cl}/n in the wavelength range, $0.01 \leq k_r \rho_{\theta i} \leq 10$.

density. Since it results from the banana orbit, it is affected by FOW effect mainly. Hence, not much difference is expected in the neoclassical polarization density when using the slowing down distribution.

The precise analytic expressions for neoclassical polarization is described as an integral of bounce-transit parameter κ and magnetic moment μ,

$$\begin{aligned}
[n_{nc,k}]_\psi &\simeq \frac{T}{T_c} n_k e^{iS(\hat{\psi})} \int |\langle e^{i\delta\zeta}\rangle_g|^2 \left(1 - |\langle e^{i\Delta\zeta}\rangle_{b,t}|^2\right) \times \left(-\frac{T\partial}{\omega_{b,t}\partial\hat{J}}\right) F_{SD}(\hat{Z}) \frac{d\hat{J}}{qR_0} \frac{Bd\hat{\mu}}{m} \\
&= \frac{T}{T_c} n_k e^{iS(\hat{\psi})} \int J_0^2\left(k_r\rho_\perp\right) \Lambda_{b,t}(\kappa; k_r\rho_{\theta\perp}) \left(-\frac{\partial}{\partial\kappa}\right) F_{SD}(\hat{Z}) d\kappa \frac{d\mu}{\mu^{1/2}\rho_i} \qquad (70)
\end{aligned}$$

where $\Lambda_{b,t}$ is normalized orbit excursion referred in the previous study [5],

$$\begin{aligned}
\Lambda_{b,t}(\kappa; k_r\rho_{\theta\perp}) &= \begin{pmatrix} 1 \\ 2 \end{pmatrix} \frac{\omega_\parallel}{\omega_{b,t}} \left(1 - |\langle e^{i\Delta\zeta}\rangle_{b,t}|^2\right) \\
&= \frac{2}{\pi} \times \begin{bmatrix} K(\kappa)\left(1 - \Sigma_{n=0}^{\infty}\Sigma_{m=0}^{n} \frac{(-1)^n \alpha^{2n}}{(2m)!(2(n-m))!} B_m B_{n-m}\right) & for\ trapped \\ \frac{K(\kappa^{-1}}{\sqrt{\kappa}}\left(1 - \Sigma_{n=0}^{\infty}\Sigma_{m=0}^{2n} \frac{(-1)^{n-m}\alpha^{2n}}{m!(2n-m)!} \kappa^n T_m T_{2n-m}\right) & for\ passing \end{bmatrix},
\end{aligned}$$

in which the function $B_m(x)$ and $T_m(x)$ is,

$$B_m(x) \equiv \kappa^m \int_{-2K(\kappa)}^{2K(\kappa)} cn^{2m}(\xi_b|\kappa)\frac{d\xi_b}{4K(\kappa)}, \tag{71}$$

$$T_m(x) \equiv \int_0^{2K(\kappa^{-1})} dn^m(\xi_t|\kappa^{-1})\frac{d\xi_t}{2K(\kappa^{-1})}. \tag{72}$$

Here, $K(\kappa)$ denotes the complete elliptic integral of the 1st kind, $\rho_{\theta\perp} = q\rho_\perp/\epsilon$ is perpendicular poloidal gyroradius, and $\alpha \equiv \sqrt{2\epsilon k_r \rho_{\theta\perp}}$. Although the expression is very delicate and precise, it is too complicate to use with the unusual distribution function like slowing down distribution. Thus, we follow the methodology of Wang and Hahm[20] and use the simplified version of the expression which is approximated in the assumption of deeply trapped limit ($\kappa \ll 1$) for the trapped regime and strongly passing limit ($\kappa \gg 1$) for the passing regime,

$$\Lambda_{b,t}(\kappa; k_r\rho_{\theta\perp}) \simeq \frac{2}{\pi} \times \begin{bmatrix} K(\kappa)\left(1 - J_0^2(\alpha\sqrt{\kappa})\right) & for\ trapped \\ \frac{K(\kappa^{-1}}{\sqrt{\kappa}}\left(1 - J_0^2\left(\alpha/4\sqrt{\kappa}\right)\right) & for\ passing \end{bmatrix}. \tag{73}$$

By doing so, we can deal with the fully analytic formula of the neoclassical polarization. Then neoclassical polarization density is calculated in three different wavelength regimes, long wavelength regime ($k_r\rho_i < k_r\rho_{\theta i} << 1$), intermediate wavelength regime ($k_r\rho_i << 1 << k_r\rho_{\theta i}$), and short wavelength regime ($1 << k_r\rho_i < k_r\rho_{\theta i}$). Details of the expressions in three regime is as follows: In the long wavelength regime, thermal gyroradius is too small to consider that FLR effect is neglected in the calculation, $J_0^2(k_r\rho) \to 1$. The effect of poloidal thermal gyroradius is also minimized but not ignored, so that only FOW effect remains in the expression, $1 - J_0^2(\alpha\sqrt{\kappa}) \to \frac{1}{2}\alpha^2\kappa$. Next, in the intermediate wavelength regime, FLR effect is still neglected but large poloidal gyroradius makes the FOW effect more effectively, $J_0^2(\alpha\sqrt{\kappa}) \to \frac{2}{\pi\alpha\sqrt{\kappa}}\cos^2(\alpha\sqrt{\kappa} - \pi/4)$. Finally, in the short wavelength regime, both FLR effect and FOW effect gets

bigger and the excursion terms get more powerful in the expression. Using some mathematical techniques and integral tables**??**, the result of the calculation is described as,

$$
\begin{aligned}
[n_{nc,k}]_{\psi}^{long} &= \frac{T}{T_c} n_{k_{nc}}^{long} \\
[n_{nc,k}]_{\psi}^{m} &= \frac{T}{T_c} n_{k_{nc}}^{m} \\
[n_{nc,k}]_{\psi}^{short} &= \frac{T}{T_c} n_{k_{nc}}^{short},
\end{aligned}
$$

where χ_{nc}^{long}, χ_{nc}^{in}, and χ_{nc}^{short} are the electric susceptibility in the range of long, intermediate, and short wavelength, respectively,

$$
\chi_{nc}^{long} = 1.63\epsilon^{3/2} k_r^2 \rho_{\theta c}^2 \tag{74}
$$

$$
\begin{aligned}
\chi_{nc}^{m} &= \frac{I_0(v_0/v_c)}{I_2(v_0/v_c)} - \frac{2\sqrt{2\epsilon}}{\pi} \frac{1}{I_2(v_0/v_c)} \sqrt{\frac{\pi}{2}} \left(1 - \frac{1}{1+(v_0/v_c)^3}\right) \Gamma'_{tr} \\
&- \left(1 - \frac{2\sqrt{2\epsilon}}{\pi}\right) \frac{1}{I_2(v_0/v_c)} \sqrt{\frac{\pi}{2}} \left(1 - \frac{1}{1+(v_0/v_c)^3}\right) \Gamma'_{p}
\end{aligned} \tag{75}
$$

$$
\begin{aligned}
\chi_{nc}^{short} &= \frac{1}{\pi k_r \rho_c} \left[\frac{1}{I_2(v_0/v_c)} \left(1 - \frac{1}{1+(v_0/v_c)^3}\right) \right. \\
&- \left. \frac{2\sqrt{2\epsilon}}{\pi} \frac{3}{I_2(v_0/v_c)} \sqrt{\frac{\pi}{2}} G(v_0/v_c) \Gamma_{tr} - \left(1 - \frac{2\sqrt{2\epsilon}}{\pi}\right) \frac{3}{I_2(v_0/v_c)} \sqrt{\frac{\pi}{2}} G(v_0/v_c) \Gamma_p \right]
\end{aligned} \tag{76}
$$

Similar with the classical polarization calculation, we construct the connection formula to complete the full version of neoclassical polarization density. In this procedure, both trapped and passing particle contribution is included. As a

result, the neoclassical polarization density is ,

$$[n_{nc,k}]_\psi = n_k \left\{ \frac{1}{\chi_{nc}^{long}} + \frac{1}{1+k_r^2\rho_c^2}\frac{1}{\chi_{nc}^{m}} + \frac{k_r^2\rho_c^2}{1+k_r^2\rho_c^2}\frac{1}{\chi_{nc}^{short}} \right\}^{-1} \tag{77}$$

It is shown in Fig.7 that the peak of neoclassical polarization density for slowing down distribution gets much lower than that for equivalent Maxwellian case in the wavelength range $k_r\rho_{\theta i} \sim 1$. And still, the values for both long and short wavelength limit is same as the Maxwellian cases.

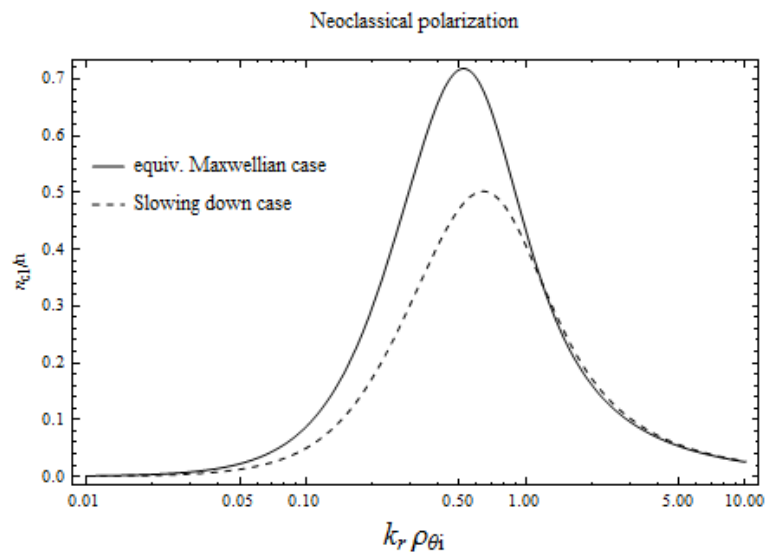

Figure 7: n_{nc}/n in the wavelength range, $0.01 \leq k_r\rho_{\theta i} \leq 10$.

4.2 Residual zonal flow level

In the previous sections, we derived the analytic expressions of the classical and neoclassical polarization density. Now, one can express the residual zonal flow level in terms of classical and neoclassical polarization density [17],

$$R_{ZF} = \frac{\phi_k(t=\infty)}{\phi_k(t=0)} = \frac{n_{cl,k}}{n_{cl,k}+n_{nc,k}} \tag{78}$$

Since classical polarization density for the slowing down distribution function gets much higher than that for the equivalent Maxwellian distribution function for wavelength on the order of poloidal gyro-radius, we expect some difference in the wavelength range, $k_r \rho_{\theta i} \sim 1$. In Fig.8, the residual zonal flow level for two different distribution functions in the Ion Temperature Gradient(ITG) turbulence with adiabatic electron shows the significant difference in the range $k_r \rho_{\theta i} \simeq 1$. One can see that the residual zonal flow level for slowing down distribution is higher than that for equivalent Maxwellian distribution, due to the enhancement of classical polarization. In other words, it is expected that the zonal flow response for the turbulence with poloidal thermal gyroradius wavelength scale gets intense in the burning plasma.

The residual level of zonal flow not only depends on the radial wavelength

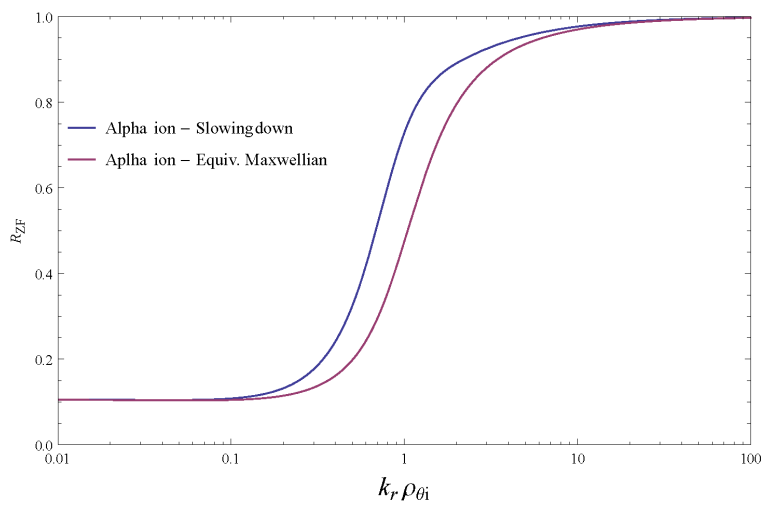

Figure 8: Residual ZF level compared with slowing down case and equivalent Maxwellian case.

but also depends on the initial particle energy when it is for slowing down distribution. It is shown in Fig.9 that normalized to the case of alpha particle energy ($E_\alpha = 3.5MeV$), the relative amplitude of residual zonal flow has a local

extremal value at the wavelength range $k_r\rho_{\theta i} \simeq 1$, and it increases as the initial particle energy decreases.

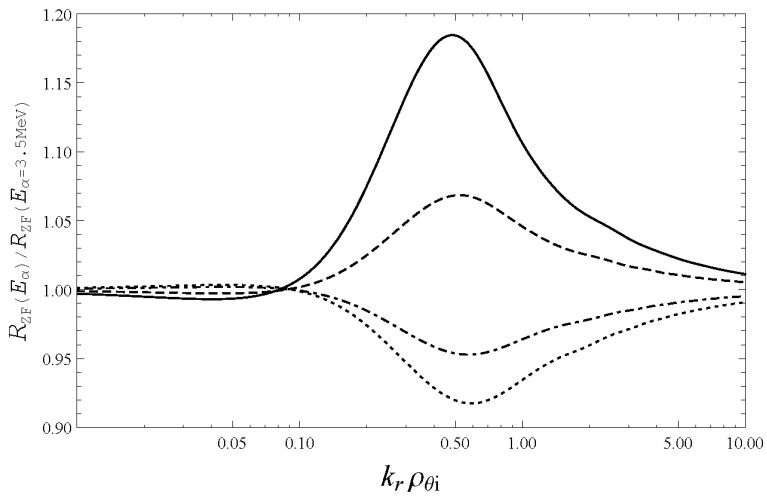

Figure 9: Relative amplitude of residual level compared with $E_\alpha = 3.5MeV$. Each line shows the result of $E_\alpha = 1.75MeV$(solid) $E_\alpha = 2.625MeV$(dashed), $E_\alpha = 4.375MeV$(dot-dashed), and $E_\alpha = 5.25MeV$(dotted) respectively.

5 Conclusions

We systematically calculate the classical and neoclassical polarization density for the slowing down equilibrium distribution via modern gyro-kinetics and bounce gyro-kinetics, respectively. In this procedure, we use flux-surface averaged quantities to see the zonal contribution to each polarization density. Also, not only the FOW but also the FLR effect are considered in the neoclassical polarization density. Because of the velocity space composition of the slowing down distribution, classical polarization density for the slowing down distribution gets much enhanced in the wavelength range, $k_r\rho_{\theta i} \sim 1$. Next, we calculate the residual zonal flow level for the arbitrary wavelength using the expressed polarization densities. We compare this result with the equivalent Maxwellian

case. It is shown that the residual level gets much higher for the wavelength range $k_r\rho_{\theta i} \sim 1$ due to the enhancement of the classical polarization density. Also, we investigate the initial particle energy dependence of residual zonal flow for slowing down distribution function and observe that the local extremum of relative zonal flow intensity occur around $k_r\rho_{\theta i} \sim 1$, and it increases as the initial particle energy decreases.

As mentioned above, residual zonal flow takes a key role for understanding the zonal flow response in the turbulent plasma. Since our focus is on the practical issues of fusion reactors, our results can be useful for the prediction of zonal flow and turbulence in the burning plasma like ITER and DEMO.

References

[1] H Biglari, PH Diamond, and PW Terry. Influence of sheared poloidal rotation on edge turbulence. *Physics of Fluids B: Plasma Physics*, 2(1):1–4, 1990.

[2] PH Diamond, SI Itoh, K Itoh, and TS Hahm. Zonal flows in plasmaa review. *Plasma Physics and Controlled Fusion*, 47(5):R35, 2005.

[3] PH Diamond and Y-B Kim. Theory of mean poloidal flow generation by turbulence. *Physics of Fluids B: Plasma Physics*, 3(7):1626–1633, 1991.

[4] Andris M Dimits, G Bateman, MA Beer, BI Cohen, W Dorland, GW Hammett, C Kim, JE Kinsey, M Kotschenreuther, AH Kritz, et al. Comparisons and physics basis of tokamak transport models and turbulence simulations. *Physics of Plasmas*, 7(3):969–983, 2000.

[5] F-X Duthoit, AJ Brizard, and TS Hahm. Compact formulas for bounce/transit averaging in axisymmetric tokamak geometry. *Physics of Plasmas*, 21(12):122510, 2014.

[6] BH Fong and TS Hahm. Bounce-averaged kinetic equations and neoclassical polarization density. *Physics of Plasmas*, 6(1):188–199, 1999.

[7] EA Frieman and Liu Chen. Nonlinear gyrokinetic equations for low-frequency electromagnetic waves in general plasma equilibria. *The Physics of Fluids*, 25(3):502–508, 1982.

[8] A Fujisawa, K Itoh, H Iguchi, K Matsuoka, S Okamura, A Shimizu, T Minami, Y Yoshimura, K Nagaoka, C Takahashi, et al. Identification of zonal flows in a toroidal plasma. *Physical review letters*, 93(16):165002, 2004.

[9] Robert J Goldston and Paul Harding Rutherford. *Introduction to plasma physics*. CRC Press, 1995.

[10] TS Hahm. Nonlinear gyrokinetic equations for tokamak microturbulence. *The Physics of fluids*, 31(9):2670–2673, 1988.

[11] TS Hahm and KH Burrell. Flow shear induced fluctuation suppression in finite aspect ratio shaped tokamak plasma. *Physics of Plasmas*, 2(5):1648–1651, 1995.

[12] RJ Hastie, JB Taylor, and FA Haas. Adiabatic invariants and the equilibrium of magnetically trapped particles. *Annals of Physics*, 41(2):302–338, 1967.

[13] FL Hinton and JA Robertson. Neoclassical dielectric property of a tokamak plasma. *The Physics of fluids*, 27(5):1243–1247, 1984.

[14] FL Hinton and MN Rosenbluth. Dynamics of axisymmetric and poloidal flows in tokamaks. *Plasma physics and controlled fusion*, 41(3A):A653, 1999.

[15] Frank Jenko, W Dorland, M Kotschenreuther, and BN Rogers. Electron temperature gradient driven turbulence. *Physics of Plasmas*, 7(5):1904–1910, 2000.

[16] Robert G Littlejohn. Hamiltonian perturbation theory in noncanonical coordinates. *Journal of Mathematical Physics*, 23(5):742–747, 1982.

[17] MN Rosenbluth and FL Hinton. Poloidal flow driven by ion-temperature-gradient turbulence in tokamaks. *Physical review letters*, 80(4):724, 1998.

[18] Thomas H Stix. Decay of poloidal rotation in a tokamak plasma. *The Physics of Fluids*, 16(8):1260–1267, 1973.

[19] Hideo Sugama and T-H Watanabe. Collisionless damping of zonal flows in helical systems. *Physics of Plasmas*, 13(1):012501, 2006.

[20] Lu Wang and TS Hahm. Generalized expression for polarization density. *Physics of Plasmas*, 16(6):062309, 2009.

[21] Yong Xiao and Peter J Catto. Plasma shaping effects on the collisionless residual zonal flow level. *Physics of plasmas*, 13(8):082307, 2006.

[22] Yong Xiao and Peter J Catto. Short wavelength effects on the collisionless neoclassical polarization and residual zonal flow level. *Physics of plasmas*, 13(10):102311, 2006.